

Towards Adversarial Robustness via Transductive Learning

Jiefeng Chen¹, Yang Guo¹, Xi Wu², Tianqi Li¹, Qicheng Lao³, Yingyu Liang¹, and Somesh Jha¹

¹University of Wisconsin-Madison

²Google

³Mila - Quebec Artificial Intelligence Institute

{jiefeng; yguo; richardl; yliang; jha}@cs.wisc.edu, wuxi@google.com,
qicheng.lao@gmail.com

Abstract

There has been emerging interest to use transductive learning for adversarial robustness (Goldwasser et al., NeurIPS 2020; Wu et al., ICML 2020). Compared to traditional “test-time” defenses, these defense mechanisms “dynamically retrain” the model based on test time input via transductive learning; and theoretically, attacking these defenses boils down to bilevel optimization, which seems to raise the difficulty for adaptive attacks. In this paper, we first formalize and analyze modeling aspects of transductive robustness. Then, we propose *the principle of attacking model space* for solving bilevel attack objectives, and present an instantiation of the principle which breaks previous transductive defenses. These attacks thus point to significant difficulties in the use of transductive learning to improve adversarial robustness. To this end, we present new theoretical and empirical evidence in support of the utility of transductive learning.

1 Introduction

Adversarial robustness of deep learning models has received significant attention in recent years (see the tutorial by [17] and references therein). The classic threat model of adversarial robustness considers an *inductive setting* where a model is trained and fixed, and an attacker attempts to thwart the model with adversarially perturbed input. This gives rise to a minimax objective for the defender, and accordingly adversarial training [23, 26, 25, 5] to improve adversarial robustness.

Going beyond the inductive model, there has been emerging interest in using *transductive learning* for adversarial robustness (Goldwasser et al. [11]; Wu et al. [33]). Basically, let U denote the clean unlabeled test-time input, and U' be the (possibly) adversarially perturbed version of U , these work apply a transductive learning algorithm Γ to U' to get an updated model $\Gamma(U')$ to predict on U' . The hope is that this test-time adaptation may be useful to improve adversarial robustness, because Γ is applied *after* the attacker’s move of producing adversarial examples U' . This scenario is practically motivated since many machine learning pipelines are deployed with batch prediction [1] ($|U'| \gg 1$).

In the first part of this work we formalize a transductive threat model to capture these defenses. From the attacker perspective, the threat model can be viewed as considering a transductive optimization objective $\max_{V' \in \mathcal{N}(V)} L_a(\Gamma(F, D, U'), V')$ (Definition 1, formula (4)), where L_a is a loss function for evaluating the gain of the attack, $U' = V'|_X$ are the test-time feature vectors, Γ is the defender mechanism, F is a pre-trained model, and D is the labeled training on which F is trained. This objective is *transductive* because U' appear in both attack (the second parameter of L_a) and defense (input to Γ).

By choosing different L_a and Γ , we show that our threat model captures various defenses, such as various test-time defenses considered in [3], Randomized Smoothing [7], as well as [11, 33]. We focus the attention of the current work in settings of [11, 33] where Γ is indeed transductive learning (by contrast, the Γ considered in [3, 7] do not update the model, but rather sanitize the input).

We then consider principles for adaptive attacks in the transductive model (principles for the inductive model have been developed in [29]). We note that with a transductive learner Γ , the attacker faces a more challenging situation: Γ is far from being differentiable (compared to the situations considered in BPDA [3]), and the attack set U' also appears in the defense Γ . To address these difficulties for adaptive attacks, our key observation is to consider the *transferability of adversarial examples*, and consider a *robust* version of (4): $\max_{U'} \min_{\bar{U} \in \mathcal{N}(U')} L_a(\Gamma(\bar{U}), V')$ (formula (8)), where we want to find a *single* attack set U' to thwart a family of models, induced by \bar{U} “around” U' . While seemingly more difficult to solve, this objective relaxes the attacker-defender constraint, and provides more information in dealing with nondifferentiability.

Based on the principle, we devise new adaptive attacks to thwart previous defenses. We show that we can break the defense in [33] in the settings of their consideration. For [11], we devise attacks against URejectron in *deep learning settings* and the *small-perturbation regime* (their theory is developed in the regime of bounded VC-dimensions) to demonstrate two subtleties: **(1)** We can generate imperceptible attacks that can slip through the discriminator trained by URejectron and cause wrong predictions, and **(2)** We can generate “benign” perturbations (for which the base classifier in URejectron predicts correctly), but will all be rejected by the discriminator. Our attacks thus point to significant difficulties in the use of transductive learning to improve adversarial robustness.

In the final part of the paper, we give new positive evidence in support of the utility of transductive learning. We propose Adversarial Training via Representation Matching (ATRM, (10)) which combines adversarial training with unsupervised domain adaptation. ATRM achieves better empirical adversarial robustness compared to adversarial training alone against our strongest attacks (on CIFAR-10, we improved from 41.06% to 53.53%). Theoretically, we prove a first separation result where with transductive learning one can obtain nontrivial robustness, while without transductive learning, no nontrivial robustness can be achieved. We also caution the limitations of these preliminary results (e.g., the high computational cost of ATRM). Nevertheless, we believe that our results give a step in systematizing the understanding of the utility of transductive learning for adversarial robustness.

2 Preliminaries

Notations. Let F be a model, and for a data point $(\mathbf{x}, y) \in \mathcal{X} \times \mathcal{Y}$, a loss function $\ell(F; \mathbf{x}, y)$ gives the loss of F on the point. Let V be a set of labeled data points, and let $L(F, V) = \frac{1}{|V|} \sum_{(\mathbf{x}, y) \in V} \ell(F; \mathbf{x}, y)$ denote the empirical loss of F on V . For example, if we use binary loss $\ell^{0,1}(F; \mathbf{x}, y) = \mathbb{1}[F(\mathbf{x}) \neq y]$, this gives the test error of F on V . We use the notation $V|_X$ to denote the projection of V to its features, that is $\{(\mathbf{x}_i, y_i)\}_{i=1}^m|_X \mapsto \{\mathbf{x}_i\}_{i=1}^m$.

Throughout the paper, we use $N(\cdot)$ to denote a neighborhood function for perturbing features: That is, $N(\mathbf{x}) = \{\mathbf{x}' \mid d(\mathbf{x}', \mathbf{x}) < \epsilon\}$ is a set of examples that are close to \mathbf{x} in terms of a distance metric d (e.g., $d(\mathbf{x}', \mathbf{x}) = \|\mathbf{x}' - \mathbf{x}\|_p$). Given $U = \{\mathbf{x}_i\}_{i=1}^m$, let $N(U) = \{\{\mathbf{x}'_i\}_{i=1}^m \mid d(\mathbf{x}'_i, \mathbf{x}_i) < \epsilon, i = 0, \dots, m\}$. Since labels are not changed for adversarial examples, we also use the notation $N(V)$ to denote perturbations of features, with labels fixed.

Dynamic models and transductive learning. Goodfellow [12] described the concept of *dynamic models*, where the model is a moving target that continually changes, even after it has been deployed. In the setting of transductive learning for adversarial robustness, this means that after the model is deployed, every time upon an (unlabeled) input test set U (potentially adversarially perturbed), the model is updated according to U before producing predictions on U . As is standard for measuring the performance of transductive learning,

we (only) measure the accuracy of the updated model on U .

Threat model for classic adversarial robustness. The classic adversarial robustness can be written down succinctly as a minimax objective, $\min_F \mathbb{E}_{(\mathbf{x}, y) \sim V} [\max_{\mathbf{x}' \in N(\mathbf{x})} [\ell(F; \mathbf{x}', y)]]$. One can reformulate this objective into a game between two players (for completeness, we record this in Definition 2 in Appendix B). This reformulation (while straightforward) is useful for formulating more complex threat models below.

3 Modeling Transductive Robustness

This section discusses modeling for transductive adversarial robustness. We first give the formal definition of our threat model, and show that it encompasses various test-time mechanisms as instantiations. We use our threat model to analyze in detail the transductive defense described in [11]. We present empirical findings for the subtleties of Goldwasser et al.’s defense in the small-perturbation regime with typical deep learning. We end this section by highlighting emphasis of this work.

3.1 Formulation of the threat model for transductive adversarial robustness

The intuition behind the transductive threat model is the same as that of the transductive learning [31], except that now the unlabeled data can be adversarially perturbed by an adversary. Specifically, at test time, after the defender receives the adversarially perturbed data U' to classify, the defender trains a model based on U' , and the test accuracy is evaluated only for U' . (i.e., for different test set U we may have different models and different test accuracy.) The formal definition is as follows:

Definition 1 (Transductive threat model for adversarial robustness). Fix an adversarial perturbation type. Let $P_{X,Y}$ be a data generation distribution. Attacker is an algorithm \mathcal{A} , and defender is a pair of algorithms (\mathcal{T}, Γ) , where \mathcal{T} is a supervised learning algorithm, and Γ is a transductive learning algorithm. Let L_a be a loss function to measure the valuation of the attack.

Before the game

Data setup

- A (clean) training set D is sampled i.i.d. from $P_{X,Y}$.
- A (clean) test set V is sampled i.i.d. from $P_{X,Y}$.

During the game

Training time

- **(Defender)** Train $F = \mathcal{T}(D)$, using the labeled source data.

Test time

- **(Attacker)** Attacker receives V , and produces an (adversarial) unlabeled dataset U' as follows:
 1. On input Γ, F, D , and V , \mathcal{A} perturbs each point $(\mathbf{x}, y) \in V$ to (\mathbf{x}', y) (subject to the agreed attack type), giving $V' = \mathcal{A}(\Gamma, F, D, V)$ (that is, $V' \in N(V)$).
 2. Send $U' = V'|_X$ (the feature vectors of V') to the defender.
- **(Defender)** Produce a model as $F^* = \Gamma(F, D, U')$.

After the game

Evaluation (referee)

The referee computes the valuation $L_a(F^*, V')$.

White-box attacks. An adversary, while cannot directly attack the final model the defender trains, still has full knowledge of the transductive mechanism Γ of the defender, and can leverage that for adaptive attacks.

Note that, however, the adversary does not know the private randomness of Γ .

Examples. The threat model is general to encompass various defenses. We give a few examples (some may not be entirely obvious).

Example 1 (Test-time defenses). *There have been numerous proposals of “test-time defenses” for adversarial robustness. These defenses can be captured by a pair (\mathcal{T}, Γ) where \mathcal{T} trains a fixed pretrained model F , and Γ is a “non-differentiable” function which sanitizes the input and then send it to Γ . Most of these proposals were broken by BPDA [3]. We note that, however, these proposals are far from transductive learning: There is no transductive learning that trains the model using the test inputs, and very often these algorithms even applied to single test points (i.e. $|U| = 1$).*

Example 2 (Randomized smoothing [7]). *Another interesting proposal that falls under our modeling is randomized smoothing. We describe the construction for $|U| = 1$, and it is straightforward to extend it to $|U| > 1$. \mathcal{T} prepares a fixed pretrained model F . Γ works as follows: Upon a test feature \mathbf{x}' , Γ samples a random string $\xi = (\varepsilon_1, \dots, \varepsilon_n)$, consisting of n independent random noises. Then Γ returns the prediction function $\text{PREDICT}[\xi]$ (PREDICT is described in “Pseudocode for certification and prediction” on top of page 5, [7]), which is PREDICT with randomness fixed. It is straightforward to check that this construction is equivalent to using PREDICT at the test time where noises are sampled internally (we simply move sampling of noises outside into Γ , and return $\text{PREDICT}[\xi]$ as a model). This is an important example for the utility of private randomness. In fact, if n is small, then an adversary can easily fail the defense for any fixed random noise.*

Neither of the two examples above uses a Γ that does “learning” on the unlabeled data. Below we analyze examples where Γ indeed does transductive learning.

Example 3 (Runtime masking and cleansing). *Runtime masking and cleansing [33] (RMC) is a recent proposal that uses test-time learning (on the unlabeled data) to enhance adversarial robustness. The Γ works with $|U| = 1$, and roughly speaking, updates the model by solving $F^* = \arg \min_F \sum_{(\mathbf{x}, y) \in N'(\hat{\mathbf{x}})} L(F, \mathbf{x}, y)$, where $\hat{\mathbf{x}}$ is the test time feature point. In this work, we develop strong adaptive attacks to break this defense.*

Example 4 (Unsupervised Domain Adaptation (as transductive learning)). *While not explored in previous work, our modeling also indicates a natural application of unsupervised domain adaptation, such as DANN [2], as transductive learning for adversarial robustness: Given U' , we train a DANN model on the training dataset D and U , and then evaluate the model on U' . In our experiments, we show that this alone already provides better robustness than RMC, even though we can still thwart this defense using our strongest adaptive attacks.*

3.2 Goldwasser et al.’s transductive threat model and URejectron

While seemingly our formulation of the transductive threat model is quite different from the one described in [11], in fact one can recover their threat model naturally (specifically, the transductive guarantee described in Section 4.2 of their paper): First, for the perturbation type, we simply allow arbitrary perturbations in the threat model setup. Second, we have a fixed pretrained model F , and the adaptation algorithm Γ learns a set S which represents the set of “allowable” points (so $F|_S$ gives the predictor with redaction, namely it outputs \perp for points outside of S). Third, we define two error functions as (5) and (6) in [11]:

$$\text{err}_{U'}(F|_S, f) \equiv \frac{1}{|U'|} \left| \left\{ \mathbf{x}' \in U' \cap S \mid F(\mathbf{x}') \neq f(\mathbf{x}') \right\} \right| \quad (1)$$

$$\text{rej}_U(S) \equiv \frac{|U \setminus S|}{|U|} \quad (2)$$

where f is the ground truth hypothesis. The first equation measures prediction errors in U' that passed through S , and the second equation measures the rejection rate of the clean input. Finally, we define the

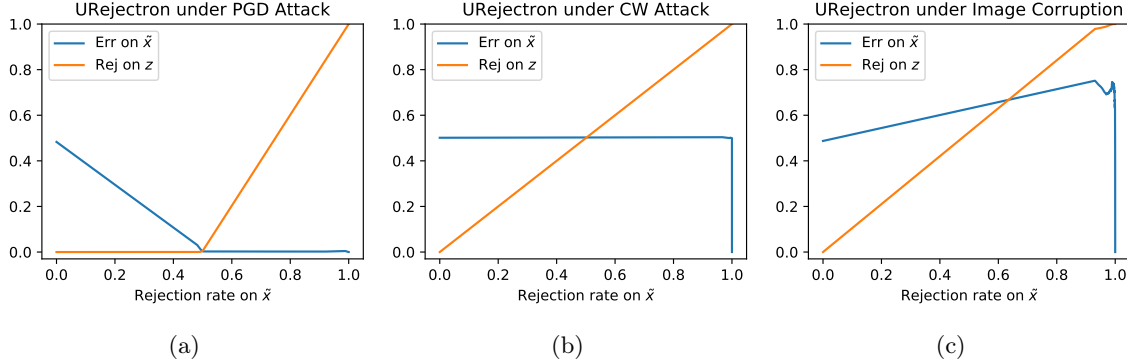


Figure 1: URejectron in three settings. z contains “normal” examples on which the classifier can have high accuracy. \tilde{x} includes z and consists of a mix of 50% “normal” examples and 50% adversarial examples. In (a), the normal examples are clean test inputs and the adversarial examples are generated by PGD attack [23]. In (b), the “normal” examples are still clean test inputs but adversarial examples are generated by CW attack [4]. In (c), the “normal” examples are generated by corruptions [15] (adversarial examples are generated by PGD attacks).

following loss function for valuation, which measures the two errors as a pair:

$$L_a(F|_S, V') = \left(\text{err}_{U'}(F|_S), \text{rej}(S) \right) \quad (3)$$

The theory in [11] is developed in the bounded VC dimension scenarios. Specifically, Theorem 5.3 of their paper (Transductive Guarantees) establishes for $\Gamma = \text{Rejectron}$ that, for proper ε^* , with high probability over $D, V \sim P_{X,Y}^n$, $L_a(\text{Rejectron}(D, U'), V') \leq (\varepsilon^*, \varepsilon^*)$, for any U' .

Subtleties of URejectron. [11] also derived an unsupervised version, URejectron, of Rejectron, with similar theoretical guarantees, and presented corresponding empirical results. Based on their implementation, we studied URejectron in the setting of *deep learning with small perturbations*. Specifically, we evaluated URejectron on GTSRB dataset using ResNet18 network. The results are shown in Figure 1. Figure 1(a) shows that for *transfer attacks* generated by PGD attack [23], URejectron can indeed work as expected. However, by using different attack algorithms, such as CW attacks [4], (nevertheless these attacks are *transfer attacks*, which are *weak* instantiations of our framework described in Section 4), we observe two possible failure modes:

Imperceptible adversarial perturbations that slip through. Figure 1(b) shows that one can construct adversarial examples that are very similar to the clean test inputs that can slip through their URejectron construction of S (in the deep learning setting), and cause large errors.

Benign perturbations that get rejected. Figure 1(c) shows that one can generate “benign” perturbed examples (i.e., the base classifier can give correct predictions), using image corruptions such as slightly increasing the brightness, but URejectron rejects them all. While strictly speaking, this failure mode is beyond their guarantee (3), this indicates that in the small-perturbation regime things can be more subtle compared to the seemingly harder “arbitrary perturbation” case.

We thus believe that a more careful consideration for the small-perturbation regime is warranted.

3.3 Focus of the current work

While we have shown that our transductive threat model formulation is quite encompassing, in this work we focus on a regime that differ from the considerations in [11]:

Small perturbations. Arbitrary perturbations include small perturbations as a special case. In this work,

we are primarily motivated to study situations where test and training samples are connected, instead of arbitrarily far away. For this reason, we focus on the *small-perturbation regime*.

Deep learning with no redaction. Due to the previous consideration, and our main motivation to study the utility of transductive learning, we focus on the case with no redaction. As for practicality considerations, we focus on deep learning, instead of learners with bounded VC dimensions.

Finally, different from test-time defenses and randomized smoothing, in this work we focus on Γ that perform actual transductive learning (i.e. update the model based on unlabeled data).

4 Adaptive Attacks against Transductive Defenses

In this section we consider adaptive attacks against transductive defenses under the *white-box* assumption: The attacker knows all the details of the defender transductive learning algorithm Γ (except private randomness used by the defender). We deduce a principle for adaptive attacks, which we call *the principle of attacking model space*: It suggests that effective attacks against a transductive defense may need to consider *attacking a small set of representative models*. We give concrete instantiations of this principle, and show in experiments that they break previous transductive defenses, and is much stronger than attacks directly adapted from literature on solving bilevel optimization objectives in deep learning.

4.1 Goal of the attacker and challenges

To start with, given a defense mechanism Γ , the objective of the attacker can be formulated as:

$$\max_{V' \in N(V), U' = V'|_X} L_a(\Gamma(F, D, U'), V'). \quad (4)$$

where L_a is the loss function of the attacker. We make some notational simplifications: Since D is a constant, in the following we drop it and write $\Gamma(U')$. Also, since the attacker does not modify the labels in the threat model, we abuse the notation (one can think as hard-wiring labels into L_a), and write the objective as

$$\max_{V', U' = V'|_X} L_a(\Gamma(U'), U'). \quad (5)$$

A generic attacker would proceed iteratively as follows: It starts with the clean test set V , and generates a sequence of (*hopefully*) *increasingly stronger* attack sets $U^{(0)} = V|_X, U^{(1)}, \dots, U^{(i)}$. We note several basic but important *differences* between transductive attacks and inductive attacks in the classic minimax threat model:

(D1) $\Gamma(U')$ is *not* differentiable. For the scenarios we are interested in, Γ is an optimization algorithm to solve an objective $F^* \in \arg \min_F L_d(F, D, U')$. This renders (5) into a bilevel optimization problem [8]:

$$\begin{aligned} & \max_{V' \in N(V); U' = V'|_X} L_a(F^*, V') \\ & \text{subject to: } F^* \in \arg \min_F L_d(F, D, U'), \end{aligned} \quad (6)$$

In these cases, Γ is in general *not* (in fact far from) differentiable. A natural attempt is to approximate Γ with a differentiable function, using theories such as Neural Tangent Kernels [16]. Unfortunately no existing theory applies to the transductive training, which deals with unlabeled data U' (also, as we have remarked previously, tricks such as BPDA [3] also does not apply because transductive learning is much more complex than test-time defenses considered there).

(D2) U' appears in *both* attack and defense. Another significant difference is that the attack set U' also appears as the input for the defense (i.e. $\Gamma(U')$). Therefore, while it is easy to find U' to fail $\Gamma(\bar{U})$ for

any fixed \bar{U} , it is much harder to find a *good direction* to update the attack and converge to *an attack set* U^* that fails an entire model space induced by itself: $\Gamma(U^*)$.

(D3) $\Gamma(U')$ can be a random variable. In the classic minimax threat model, the attacker faces a fixed model. However, the output of Γ can be a *random variable of models* due to its private randomness, such as the case of Randomized Smoothing (Example 2). In these cases, successfully attacking a single sample of this random variable does not suffice.

Algorithm 1 FIXED POINT ATTACK (FPA)

Require: A transductive learning algorithm Γ , an optional training dataset D , a natural test dataset V , an initial model $F^{(0)}$, and an integer parameter $T \geq 0$ (the number of iterations).

- 1: **for** $i = 0, 1, \dots, T$ **do**
- 2: Attack the model obtained in the last iteration to get the perturbed set:

$$V^{(i)} = \operatorname{argmax}_{V' \in \mathcal{N}(V)} L_a(F^{(i)}, V') \quad (7)$$

where L_a is the standard test loss. Set $U^{(i)} = V^{(i)}|_X$.

- 3: Run the transductive learning algorithm Γ to get the next model: $F^{(i+1)} = \Gamma(D, U^{(i)})$.
 - 4: **end for**
 - 5: Select the best attack set $U^{(k)}$ as $k = \operatorname{argmax}_{0 \leq i \leq T} L_a(F^{(i+1)}, V^{(i)})$.
 - 6: **return** $U^{(k)}$.
-

Fixed Point Attack: A first attempt. We adapt previous literature for solving bilevel optimization in deep learning setting [22] (designed for supervised learning). The idea is simple: At iteration $i + 1$, we fix $U^{(i)}$ and model space $F^{(i)} = \Gamma(U^{(i)})$, and construct $U^{(i+1)}$ to fail it. We call this the Fixed Point Attack (FPA), as one hopes that this process converges to a good fixed point U^* . Unfortunately, we found FPA to be weak in experiments. The reason is exactly **(D2)**: $U^{(i+1)}$ failing $F^{(i)}$ may not give any indication that it can also fail $F^{(i+1)}$ induced by itself.

4.2 Strong adaptive attacks from attacking model spaces

To develop stronger adaptive attacks, we consider a key property of the adversarial attacks: The *transferability of adversarial examples*. Various previous work have identified that adversarial examples transfer [30, 21], even across vastly different architectures and models. Therefore, if U' is a good attack set, we would expect that U' also fails $\Gamma(\bar{U})$ for \bar{U} close to U' . This leads to the consideration of the following objective:

$$\max_{U'} \min_{\bar{U} \in \mathcal{N}(U')} L_a(\Gamma(\bar{U}), U'). \quad (8)$$

where $\mathcal{N}(\cdot)$ is a neighborhood function (possibly different than N). It induces a family of models $\{\Gamma(U') \mid U' \in \mathcal{N}(U^*)\}$, which we call a *model space*. (in fact, this can be a family of random variables of models) This can be viewed as a natural *robust* version of (5) by considering the transferability of U' . While this is seemingly even harder to solve, it has several benefits:

(1) Considering a model space naturally strengthens FPA. FPA naturally falls into this formulation as a weak instantiation where we consider a single $\bar{U} = U^{(i)}$. Also, considering a model space gives the attacker more information in dealing with the nondifferentiability of Γ **(D1)**.

(2) It relaxes the attacker-defender constraint (D2). Perhaps more importantly, for the robust objective, we no longer need the same U' to appear in both defender and attacker. Therefore it gives a natural relaxation which makes attack algorithm design easier.

In summary, while “brittle” U' that does not transfer may indeed exist theoretically, their identification can be challenging algorithmically, and its robust variant provides a natural relaxation considering both algorithmic feasibility and attack strength. This thus leads us to the following principle:

The Principle of Attacking Model Spaces. *An efficient and effective adaptive attack strategy against a transductive defense may need to consider a model space induced by different \bar{U} 's, and then identify an attack set to fail all of them.*

Algorithm 2 GREEDY MODEL SPACE ATTACK (GMSA)

Require: A transductive learning algorithm Γ , an optional training dataset D , a natural test dataset V , an initial model $F^{(0)}$, and an integer parameter $T \geq 0$ (the number of iterations).

- 1: **for** $i = 0, 1, \dots, T$ **do**
- 2: Attack the previous models to get the perturbed set:

$$V^{(i)} = \operatorname{argmax}_{V' \in \mathcal{N}(V)} L_{\text{GMSA}}(\{F^{(j)}\}_{j=0}^i, V') \tag{9}$$

where L_{GMSA} is a loss function. Set $U^{(i)} = V^{(i)} \upharpoonright_X$.

- 3: Run the transductive learning algorithm Γ to get the next model: $F^{(i+1)} = \Gamma(D, U^{(i)})$.
 - 4: **end for**
 - 5: Select the best attack $U^{(k)}$ as $k = \operatorname{argmax}_{0 \leq i \leq T} L_a(F^{(i+1)}, V^{(i)})$,
 - 6: **return** $U^{(k)}$.
-

An instantiation: Greedy Model Space Attack (GMSA). We give a simplest possible instantiation of the principle, which we call the *Greedy Model Space Attack* (Algorithm 2). In experiments we use this instantiation to break previous defenses. In this instantiation, the family of model spaces to consider is just all the model spaces constructed in previous iterations (line 2). L_{GMSA} (9) is a loss function that the attacker uses to attack the history model spaces. We consider two instantiations: (1) $L_{\text{GMSA}}^{\text{AVG}}(\{F^{(j)}\}_{j=0}^i, V') = \frac{1}{i+1} \sum_{j=0}^i L(F^{(j)}, V')$, (2) $L_{\text{GMSA}}^{\text{MIN}}(\{F^{(j)}\}_{j=0}^i, V') = \min_{0 \leq j \leq i} L(F^{(j)}, V')$, where $L_{\text{GMSA}}^{\text{AVG}}$ gives attack algorithm GMSA-AVG, and $L_{\text{GMSA}}^{\text{MIN}}$ gives attack algorithm GMSA-MIN. We solve (9) via Projected Gradient Decent (PGD) (the implementation details of GMSA can be found in Appendix D.1.3).

5 New Positive Evidence for the Usefulness of Transductive Learning

In the experiments we will show that the new adaptive attacks devised in this paper breaks previous defenses (in typical deep learning settings). This thus points to significant difficulties in the use of transductive learning to improve adversarial robustness. To this end, we provide new positive evidence: Empirically, we show that by combining adversarial training and unsupervised domain adaptation (ATRM), one can indeed obtain improved adversarial robustness compared to adversarial training alone, against our strongest attacks. Theoretically, we prove a separation result which demonstrates the utility of transductive learning. We caution the limitations of these preliminary results, such as the high computational cost of ATRM. Nevertheless, these represent a step to systematize the understanding of the utility of transductive learning for adversarial robustness.

5.1 Adversarial Training via Representation Matching (ATRM)

We consider a transductive learning version of adversarial training where we not only perform adversarial training but also align the representations of the adversarial training examples and the given test inputs. Specifically, we consider models $F(\mathbf{x}) = c(\phi(\mathbf{x}))$ that is a composition of a prediction function c and a

representation function ϕ . We propose to train the dynamic model with the following objective:

$$\begin{aligned} & \underset{F}{\text{minimize}} \quad \mathbb{E}_{(\mathbf{x}', y) \in D'} [\ell(F(\mathbf{x}'), y)] + \alpha \cdot d(p_{D'}^\phi, p_{U'}^\phi) \\ & \text{where } D' = \underset{D' \in N(D)}{\text{argmax}} \quad \mathbb{E}_{(\mathbf{x}', y) \in D'} \ell(F(\mathbf{x}'), y) \end{aligned} \tag{10}$$

where $N(D)$ is a collection of perturbed sets of D and $d(p_{D'}^\phi, p_{U'}^\phi)$ is the distance between the distribution of $\phi(\mathbf{x})$ on D' and that on U' . This method, named as Adversarial Training via Representation Matching (ATRM), achieves positive results in our experiments in Section 6.

5.2 Transductive vs. Inductive: A Separation Result

We now turn to new theoretical evidence about the usefulness of transductive learning. A basic theoretical question is *whether the transductive setting allows better defense than the traditional inductive setting*. We observe that, by the max–min inequality, the defender’s game value in the former is *no worse* than that in the latter (see Appendix C.1 for proofs). While this conclusion doesn’t involve algorithms, we also observe that the same holds when algorithms are considered: Any defense algorithm in the inductive setting can be used as an adaptation algorithm Γ in the transductive setting (which simply ignores the test inputs and outputs the model trained on the training data), and obtains *no worse* results. However, these observations only imply that the transductive defense is no harder, but does not imply that it can be strictly better.

A separation result. We thus consider a further question: *Are there problem instances for which there exist defense algorithms in the transductive setting with strictly better performance than any algorithm in the inductive setting?* Here a problem instance is specified by a family of data distributions $P_{X,Y}$, the feasible set of the adversarial perturbations, the number of training data points, and the number of test inputs for the transductive setting. We answer this positively by constructing such problem instances (see Appendix C.2 for proofs):

Theorem 1. *For any $\epsilon \in (0, \frac{1}{3})$, there exist problem instances of binary classification with 0-1 loss:*

- (1) *In the inductive threat setting, the learned model by any algorithms must have a large loss at least $\frac{1}{2}(1 - \epsilon)$.*
- (2) *In the transductive threat setting, there exist polynomial-time algorithms \mathcal{T} and Γ such that the adapted model has a small loss at most ϵ .*

It is an intriguing direction to generalize this result to a broader class of problems.

6 Experiments

This section evaluates several transductive-learning based defenses. Our findings are summarized as follows (Appendix D gives details for replicating results): **(1)** Using Fixed Point Attack (FPA), one can already thwart RMC [33]. **(2)** For transductive defenses that are robust to FPA (e.g. RMC⁺ and DANN), the GMSA can thwart them. **(3)** Our ATRM defense provides significant improvement in adversarial robustness, compared to the adversarial training alone, against our strongest attacks. For all experiments, the defender uses his own private randomness, which is different from the one used by the attacker. Without specified otherwise, all reported values are percentages.

Dataset	Model	Accuracy	Robustness			
			PGD	FPA	GMSA-AVG	GMSA-MIN
MNIST	Standard	99.00	98.30	0.60	0.50	1.10
	Madry et al.	97.00	96.10	59.50	61.40	58.80
CIFAR-10	Standard	93.10	97.60	8.50	8.00	8.10
	Madry et al.	90.90	71.70	40.80	42.50	39.60

Table 1: Results on RMC. The PGD attack the one used in [33].

Dataset	Model	Method	Robustness			
			PGD-skip	FPA	GMSA-AVG	GMSA-MIN
MNIST	Standard	RMC	0.70	0.10	0.00	0.00
		RMC ⁺	89.60	80.70	27.10	3.40
	Madry et al.	RMC	6.40	3.70	0.40	0.10
		RMC ⁺	85.50	69.80	9.60	4.00
CIFAR-10	Standard	RMC	0.40	0.10	0.00	0.00
		RMC ⁺	75.10	60.70	17.60	4.80
	Madry et al.	RMC	34.80	33.10	21.60	16.80
		RMC ⁺	81.50	71.70	37.30	23.50

Table 2: Results on RMC and RMC⁺ under the PGD-skip attack setting. We set $p = 100$.

6.1 Attacking Runtime Masking and Cleansing Defense

Runtime masking and cleansing (RMC) [33]. RMC claimed to achieve state-of-the-art robustness under several adversarial attacks. However, those attacks are not adaptive attacks since the attacker is unaware of the defense mechanism. We thus evaluate RMC with our adaptive attacks. We assume that the attacker can simulate the adaptation process to generate a sequence of adversarial examples for evaluation. The results are in Table 1: RMC with the standard model is already broken by FPA attack (which is weaker than GSMA). Compared to the defense-unaware PGD attack, our GMSA-AVG attack reduces the robustness from 98.30% to 0.50% on MNIST and from 97.60% to 8.00% on CIFAR-10. Further, RMC with adversarially trained model actually provides *worse* adversarial robustness than using adversarial training alone. Under our GMSA-MIN attack, the robustness is reduced from 96.10% to 58.80% on MNIST and from 71.70% to 39.60% on CIFAR-10.

RMC and RMC⁺ (an extension of RMC) under the PGD-skip attack setting proposed in [33].

In this setting, the attacker generates an adversarial example $\hat{\mathbf{x}}^{(p+1)}$ against the network that has been adapted to $\hat{\mathbf{x}}^{(1)}, \dots, \hat{\mathbf{x}}^{(p)}$. (we did not consider the weakened versions of PGD-skip attack, such as PGD-Skip-Partial and PGD-Skip-Delayed attacks, since they are weaker than PGD-skip and they actually limit the attacker’s power in the white-box setting). The results are in Table 2: As observed in [33], under PGD-skip attack, RMC provides limited robustness, while RMC⁺ achieves good robustness. Also, we find that RMC⁺ is also somewhat robust under the FPA attack. However, our GMSA-MIN attack (which is stronger than both PGD-skip and FPA attacks), breaks both RMC and RMC⁺. For example, on MNIST, GMSA-MIN attack reduces the robustness of RMC⁺ with adversarially trained model from 69.80% to 4.00%. On CIFAR-10, the robustness of RMC⁺ with standard model is reduced from 60.70% to 4.80% and the robustness of RMC⁺ with adversarially trained model is reduced from 71.70% to 23.50% (which is worse than adversarial training alone).

6.2 Unsupervised Domain Adaptation and ATRM

Attacking DANN. We also evaluate DANN (alone) as a transductive learning mechanism for adversarial robustness. The results are presented in Table 3. Interestingly, DANN can provide non-trivial adversarial

Dataset	Setting	Method	Accuracy	Robustness			
				PGD	FPA	GMSA-AVG	GMSA-MIN
MNIST	Inductive	Standard	99.42	0.00	-	-	-
		Madry et al.	99.16	91.61	-	-	-
	Transductive	DANN	99.27	96.66	96.81	79.37	6.17
		ATRM	99.02	95.55	95.15	94.32	95.22
CIFAR-10	Inductive	Standard	93.95	0.00	-	-	-
		Madry et al.	86.06	41.06	-	-	-
	Transductive	DANN	92.05	54.29	8.55	0.51	0.08
		ATRM	85.11	60.71	61.59	53.53	57.66

Table 3: Results of DANN and ATRM, and comparisons with the baselines in the inductive setting. For fair comparison, different learning methods share the same model architecture and basic training configuration. The PGD attack for DANN and ATRM is the transfer attack.

robustness under the transfer attack and even the FPA attack (which is better than RMC). However, it is broken by our GMSA-MIN attack. For example, on MNIST, the robustness is reduced from 96.66% to 6.17%, and on CIFAR-10, the robustness is reduced from 8.55% to 0.08%.

Effects of combining adversarial training with UDA. Table 3 report results for ATRM. Under our strongest adaptive attacks, ATRM still provides significant adversarial robustness, and improves over *adversarial training alone*: On MNIST, ATRM improves the robustness from 91.61% to 94.32%; on CIFAR-10, it improves from 41.06% to 53.53%. These encouraging results suggest further exploration of the utility of transductive learning for adversarial robustness is warranted.

References

- [1] Online versus batch prediction. <https://cloud.google.com/ai-platform/prediction/docs/online-vs-batch-prediction>, 2021.
- [2] Hana Ajakan, Pascal Germain, Hugo Larochelle, François Laviolette, and Mario Marchand. Domain-adversarial neural networks. *stat*, 1050:15, 2014.
- [3] Anish Athalye, Nicholas Carlini, and David A. Wagner. Obfuscated gradients give a false sense of security: Circumventing defenses to adversarial examples. In Jennifer G. Dy and Andreas Krause, editors, *Proceedings of the 35th International Conference on Machine Learning, ICML 2018, Stockholm, Sweden, July 10-15, 2018*, volume 80 of *Proceedings of Machine Learning Research*, pages 274–283. PMLR, 2018.
- [4] Nicholas Carlini and David A. Wagner. Towards evaluating the robustness of neural networks. In *2017 IEEE Symposium on Security and Privacy, SP 2017, San Jose, CA, USA, May 22-26, 2017*, pages 39–57. IEEE Computer Society, 2017.
- [5] Yair Carmon, Aditi Raghunathan, Ludwig Schmidt, John C Duchi, and Percy S Liang. Unlabeled data improves adversarial robustness. In *Advances in Neural Information Processing Systems*, pages 11190–11201, 2019.
- [6] Ching-Yao Chuang, Antonio Torralba, and Stefanie Jegelka. Estimating generalization under distribution shifts via domain-invariant representations. In *Proceedings of the 37th International Conference on Machine Learning, ICML 2020, 13-18 July 2020, Virtual Event*, volume 119 of *Proceedings of Machine Learning Research*, pages 1984–1994. PMLR, 2020.
- [7] Jeremy M. Cohen, Elan Rosenfeld, and J. Zico Kolter. Certified adversarial robustness via randomized smoothing. In Kamalika Chaudhuri and Ruslan Salakhutdinov, editors, *Proceedings of the 36th International Conference on Machine Learning, ICML 2019, 9-15 June 2019, Long Beach, California, USA*, volume 97 of *Proceedings of Machine Learning Research*, pages 1310–1320. PMLR, 2019.
- [8] Benoît Colson, Patrice Marcotte, and Gilles Savard. An overview of bilevel optimization, 2007.

- [9] Francesco Croce and Matthias Hein. Reliable evaluation of adversarial robustness with an ensemble of diverse parameter-free attacks. In *Proceedings of the 37th International Conference on Machine Learning, ICML 2020, 13-18 July 2020, Virtual Event*, volume 119 of *Proceedings of Machine Learning Research*, pages 2206–2216. PMLR, 2020.
- [10] Yaroslav Ganin, Evgeniya Ustinova, Hana Ajakan, Pascal Germain, Hugo Larochelle, François Laviolette, Mario Marchand, and Victor S. Lempitsky. Domain-adversarial training of neural networks. *J. Mach. Learn. Res.*, 17:59:1–59:35, 2016.
- [11] Shafi Goldwasser, Adam Tauman Kalai, Yael Tauman Kalai, and Omar Montasser. Beyond perturbations: Learning guarantees with arbitrary adversarial test examples. *CoRR*, abs/2007.05145, 2020.
- [12] Ian J. Goodfellow. A research agenda: Dynamic models to defend against correlated attacks. *CoRR*, abs/1903.06293, 2019.
- [13] Ian J. Goodfellow, Jonathon Shlens, and Christian Szegedy. Explaining and harnessing adversarial examples. In Yoshua Bengio and Yann LeCun, editors, *3rd International Conference on Learning Representations, ICLR 2015, San Diego, CA, USA, May 7-9, 2015, Conference Track Proceedings*, 2015.
- [14] Kaiming He, Xiangyu Zhang, Shaoqing Ren, and Jian Sun. Deep residual learning for image recognition. In *2016 IEEE Conference on Computer Vision and Pattern Recognition, CVPR 2016, Las Vegas, NV, USA, June 27-30, 2016*, pages 770–778. IEEE Computer Society, 2016.
- [15] Dan Hendrycks and Thomas G. Dietterich. Benchmarking neural network robustness to common corruptions and perturbations. In *7th International Conference on Learning Representations, ICLR 2019, New Orleans, LA, USA, May 6-9, 2019*. OpenReview.net, 2019.
- [16] Arthur Jacot, Franck Gabriel, and Clement Hongler. Neural tangent kernel: Convergence and generalization in neural networks. In S. Bengio, H. Wallach, H. Larochelle, K. Grauman, N. Cesa-Bianchi, and R. Garnett, editors, *Advances in Neural Information Processing Systems*, volume 31. Curran Associates, Inc., 2018.
- [17] Zico Kolter and Aleksander Madry. Adversarial Robustness - Theory and Practice. <https://adversarial-ml-tutorial.org/>, 2018.
- [18] Alex Krizhevsky, Geoffrey Hinton, et al. Learning multiple layers of features from tiny images. 2009.
- [19] Alexey Kurakin, Ian J. Goodfellow, and Samy Bengio. Adversarial examples in the physical world. In *5th International Conference on Learning Representations, ICLR 2017, Toulon, France, April 24-26, 2017, Workshop Track Proceedings*. OpenReview.net, 2017.
- [20] Yann LeCun. The mnist database of handwritten digits. <http://yann.lecun.com/exdb/mnist/>, 1998.
- [21] Yanpei Liu, Xinyun Chen, Chang Liu, and Dawn Song. Delving into transferable adversarial examples and black-box attacks. *CoRR*, abs/1611.02770, 2016.
- [22] Jonathan Lorraine and David Duvenaud. Stochastic hyperparameter optimization through hypernetworks. *CoRR*, abs/1802.09419, 2018.
- [23] Aleksander Madry, Aleksandar Makelov, Ludwig Schmidt, Dimitris Tsipras, and Adrian Vladu. Towards deep learning models resistant to adversarial attacks. In *6th International Conference on Learning Representations, ICLR 2018, Vancouver, BC, Canada, April 30 - May 3, 2018, Conference Track Proceedings*. OpenReview.net, 2018.
- [24] Seyed-Mohsen Moosavi-Dezfooli, Alhussein Fawzi, and Pascal Frossard. Deepfool: A simple and accurate method to fool deep neural networks. In *2016 IEEE Conference on Computer Vision and Pattern Recognition, CVPR 2016, Las Vegas, NV, USA, June 27-30, 2016*, pages 2574–2582. IEEE Computer Society, 2016.
- [25] Ludwig Schmidt, Shibani Santurkar, Dimitris Tsipras, Kunal Talwar, and Aleksander Madry. Adversarially robust generalization requires more data. In *Advances in Neural Information Processing Systems*, pages 5014–5026, 2018.
- [26] Aman Sinha, Hongseok Namkoong, and John C. Duchi. Certifying some distributional robustness with principled adversarial training. In *6th International Conference on Learning Representations, ICLR 2018, Vancouver, BC, Canada, April 30 - May 3, 2018, Conference Track Proceedings*. OpenReview.net, 2018.

- [27] Johannes Stalkamp, Marc Schlipf, Jan Salmen, and Christian Igel. Man vs. computer: Benchmarking machine learning algorithms for traffic sign recognition. *Neural Networks*, 32:323–332, 2012.
- [28] Yu Sun, Xiaolong Wang, Liu Zhuang, John Miller, Moritz Hardt, and Alexei A. Efros. Test-time training with self-supervision for generalization under distribution shifts. In *ICML*, 2020.
- [29] Florian Tramèr, Nicholas Carlini, Wieland Brendel, and Aleksander Madry. On adaptive attacks to adversarial example defenses. In Hugo Larochelle, Marc’Aurelio Ranzato, Raia Hadsell, Maria-Florina Balcan, and Hsuan-Tien Lin, editors, *Advances in Neural Information Processing Systems 33: Annual Conference on Neural Information Processing Systems 2020, NeurIPS 2020, December 6-12, 2020, virtual*, 2020.
- [30] Florian Tramèr, Nicolas Papernot, Ian Goodfellow, Dan Boneh, and Patrick McDaniel. The space of transferable adversarial examples. *arXiv*, 2017.
- [31] Vladimir Vapnik. *Statistical learning theory*. Wiley, 1998.
- [32] Dequan Wang, Evan Shelhamer, Shaoteng Liu, Bruno Olshausen, and Trevor Darrell. Tent: Fully test-time adaptation by entropy minimization. In *International Conference on Learning Representations*, 2021.
- [33] Yi-Hsuan Wu, Chia-Hung Yuan, and Shan-Hung Wu. Adversarial robustness via runtime masking and cleansing. In *Proceedings of the 37th International Conference on Machine Learning, ICML 2020, 13-18 July 2020, Virtual Event*, volume 119 of *Proceedings of Machine Learning Research*, pages 10399–10409. PMLR, 2020.
- [34] Hongyang Zhang, Yaodong Yu, Jiantao Jiao, Eric P. Xing, Laurent El Ghaoui, and Michael I. Jordan. Theoretically principled trade-off between robustness and accuracy. In Kamalika Chaudhuri and Ruslan Salakhutdinov, editors, *Proceedings of the 36th International Conference on Machine Learning, ICML 2019, 9-15 June 2019, Long Beach, California, USA*, volume 97 of *Proceedings of Machine Learning Research*, pages 7472–7482. PMLR, 2019.

Supplementary Material

Towards Adversarial Robustness via Transductive Learning

We introduce the related work in Section A and the threat model for classic adversarial robustness in Section B. In Section C, we present our theoretical results on transductive defenses and their proofs. In Section D, we describe the detailed settings for the experiments and also present some additional experimental results.

A Related Work

This paper presents an interplay between three research directions: Adversarial robustness, transductive learning, and domain adaptation.

Adversarial robustness in the inductive setting. Many attacks have been proposed to evaluate the adversarial robustness of the defenses in the inductive setting where the model is fixed during the evaluation phase [13, 4, 19, 24, 9]. Principles for adaptive attacks have been developed in [29] and many existing defenses are shown to be broken based on attacks developed from these principles [3]. A fundamental method to obtain adversarial robustness in this setting is adversarial training [23, 34].

Adversarial robustness in the transductive setting. There have been emerging interests in researching dynamic model defenses in the transductive setting. A research agenda for dynamic model defense has been proposed [12]. [33] proposed the first defense method called RMC under this setting to improve the adversarial robustness of a model after deployment. However, their attacks for evaluation are somewhat weak according to our principle of attacking model space for transductive defense and in this work, we show that one can indeed break their transductive defense by attacking model space.

Domain adaptation methods. Domain adaptation is a set of techniques for training models where the target domain differs from the source. DANN [2] is a classic technique for unsupervised domain adaptation (UDA) where we have access to unlabeled test data. In this work, we propose a novel use of DANN as a transductive defense method. We showed that DANN alone is susceptible to model space attacks, but gives a nontrivial improvement of adversarial robustness when combined with adversarial training.

Test-time adaptation methods. Test-time adaptation is a recent paradigm to further improve the efficiency for adapting to novel domains [32, 28]. However, these methods are not designed to achieve adversarial robustness and we find that they are vulnerable even under the transfer attacks.

B Threat Model for Classic Adversarial Robustness

Definition 2 (Threat model for classic adversarial robustness). Attacker and defender agree on a particular attack type. Attacker is an algorithm \mathcal{A} , and defender is a supervised learning algorithm \mathcal{T} .

Before the game

Data setup

- A (labeled) training set D is sampled i.i.d. from (X, Y) .

During the game

Training time

- (**Defender**) Train a model F on D as $F = \mathcal{T}(D)$.

Test time

- A (labeled) natural test set V is sampled i.i.d. from (X, Y) .
- (**Attacker**) On input F , D , and V , \mathcal{A} perturbs each point $(x, y) \in V$ to (x', y) (subject to the agreed attack type, i.e. $x' \in N(x)$), giving $\tilde{V} = \mathcal{A}(F, D, V)$.

After the game

Evaluation (referee)

Evaluate the test loss of F on \tilde{V} , $L(F, \tilde{V})$. Attacker's goal is to maximize the test loss, while the defender's goal is to minimize the test loss.

C Theoretical Results on Transductive Defenses

C.1 Valuation of the Game

Proposition 1 (maximin vs. classic minimax threat model). Let $k \geq 1$ be a natural number, and \mathcal{F} be the hypothesis class. For a given V , the domain of \tilde{V} is a well-defined function of V (e.g., ℓ_∞ ball around V). We have that: $\mathbb{E}_{V \sim (X, Y)^k} \left[\max_U \min_{\tilde{F} \in \mathcal{F}} \{L(\tilde{F}, \tilde{V})\} \right] \leq \min_{\tilde{F} \in \mathcal{F}} \mathbb{E}_{V \sim (X, Y)^k} \left[\max_{\tilde{V}} \{L(\tilde{F}, \tilde{V})\} \right]$

Proof. Let \mathcal{F} be the family of models \tilde{F} we can choose from. From the maximin inequality, we have that

$$\max_U \min_{\tilde{F} \in \mathcal{F}} \{L(\tilde{F}, \tilde{V})\} \leq \min_{\tilde{F} \in \mathcal{F}} \max_{\tilde{V}} \{L(\tilde{F}, \tilde{V})\}$$

Note that for the minimax, the max over \tilde{V} is also constrained to perturb features (as we want to find adversarial examples). If we take expectation over V , we have then

$$\mathbb{E}_V \left[\max_U \min_{\tilde{F} \in \mathcal{F}} \{L(\tilde{F}, \tilde{V})\} \right] \leq \mathbb{E}_V \left[\min_{\tilde{F} \in \mathcal{F}} \max_{\tilde{V}} \{L(\tilde{F}, \tilde{V})\} \right]$$

Note that

$$\mathbb{E}_V \left[\min_{\tilde{F} \in \mathcal{F}} \max_{\tilde{V}} \{L(\tilde{F}, \tilde{V})\} \right] \leq \min_{\tilde{F} \in \mathcal{F}} \mathbb{E}_V \left[\max_{\tilde{V}} \{L(\tilde{F}, \tilde{V})\} \right],$$

which completes the proof. □ □

The proof holds verbatim to the more general semi-supervised threat model. We also note that, in fact, if the concept class has unbounded VC dimension, then good models always *exist* that can fit both D and V perfectly. So the valuation of the maximin game is actually always 0:

Proposition 2 (Good models exist with large capacity). Consider binary classification tasks and that the hypothesis class \mathcal{F} has infinite VC dimension. Then the valuation of the maximin game

$$\mathbb{E}_{V \sim (X, Y)^k} \left[\max_U \min_{\tilde{F} \in \mathcal{F}} \{L(\tilde{F}, \tilde{V})\} \right] \quad (11)$$

is 0. That is, perfect models always exist to fit U .

This thus gives a first evidence that that transductive adversarial learning is strictly easier. We remark that transductive learning here is essential (different models are allowed for different U). We conclude this section by noting the following:

Proposition 3 (Good minimax solution is also a good maximin solution). Suppose \mathcal{T}^* is a supervised learning algorithm which trains a model $F^* = \mathcal{T}^*(D)$, where its adversarial gain in the adversarial semi-supervised minimax model is bounded by κ (i.e. $\mathbb{E}_{V'}[\max_{\tilde{V}} L(F^*, \tilde{V})] \leq \kappa$.) Then in the maximin threat model, the adversarial gain of the strategy $(\mathcal{T}^*, \Gamma^*)$, where $\Gamma^*(F^*, D, U) = F^* = \mathcal{T}^*(D)$, is also upper bounded by κ .

C.2 Usefulness of transductive learning

Having defined the transductive adversarial threat model, a natural next question is thus to examine the relationship between our threat model and the classic inductive threat model. A standard way to study this question is via the valuation of the respective games, where in the transductive threat model it is a maximin game, and in the inductive model it is a minimax game. To this end, by standard arguments, we get immediate results such as the transductive model is no harder than the inductive threat model. We collect these results in Appendix C.1.

We note, however, that valuation of the game does *not* give any insight for the existence of good *transductive* defense algorithms, which can only leverage unlabeled data. In this section we provide a problem instance (i.e., data distributions and number of data points), and prove that that transductive threat model is *strictly easier* than the inductive threat model for the problem: *In the inductive model no algorithm can achieve a nontrivial error, while in the transductive model there are algorithms achieving small errors.* Since the transductive model is no harder than the inductive model for all problem instances, and there is a problem instance where the former is strictly easier, we thus formally establish a separation between the two threat models. Furthermore, the problem instance we considered is on Gaussian data. The fact that transductive model is already strictly easier than inductive in this simple problem provides positive support for potentially the same phenomenon on more complicated data.

Data distributions and the learning task. We consider the homogeneous case (the source and target are the same distribution) and the ℓ_∞ attack. We consider the classic Gaussian data model recently used for analyzing adversarial robustness in [25, 5]: A binary classification task where $\mathcal{X} = \mathbb{R}^d$ and $\mathcal{Y} = \{+1, -1\}$, y uniform on \mathcal{Y} and $x|y \sim \mathcal{N}(y\mu, \sigma^2 I)$ for a vector $\mu \in \mathbb{R}^d$ with $\|\mu\|_2^2 = d$ and coordinate noise variance $\sigma^2 > 0$. In words, this is a mixture of two Gaussians, one with label +1, and one with label -1. For both threat models, the datasets $D = \{(x_i, y_i)\}_{i=1}^n$ and $V = \{(x, y)\}$. In particular, V only has one data point. In the transductive threat model, we let x' denote the perturbed input obtained from x by the ℓ_∞ attack with bounded norm $\epsilon > 0$, i.e., $x' = x + \nu$ with $\|\nu\|_\infty \leq \epsilon$. Put $\tilde{V} = \{(x', y)\}$ and $U = \{x'\}$. We prove the following:

Theorem 2 (Separation of transductive and inductive threat models). There exists absolute constants $C_1, C_2, c, C > 0$ such that for any $\nu \in (0, 1)$, if $\sigma^2 = C_1 \sqrt{d \log \frac{1}{\nu}}$, $\frac{d}{\log^2 d} \geq C_2 \left(\frac{1}{\nu} + \frac{1}{\epsilon^4} \log^3 \frac{1}{\nu}\right)$, and $c \log^2 \frac{1}{\nu} \leq n \leq \frac{C\epsilon^2}{\log d} \sqrt{d \log \frac{1}{\nu}}$ in the above data model, then:¹

¹The bound on d makes sure the range of n is not empty. The expectation of the error is over the randomness of D, V, V' , and possible algorithm randomness.

- (1) In the inductive threat model, the learned model $\tilde{F} = \Gamma(\mathcal{T}(D), D, U)$ by any algorithms \mathcal{T} and Γ must have a large error: $\mathbb{E} \left\{ L(\tilde{F}, \tilde{V}') \right\} \geq \frac{1}{2}(1 - \nu)$.
- (2) In the transductive threat model, there exist \mathcal{T} and Γ such that the adapted model $\tilde{F} = \Gamma(\mathcal{T}(D), D, U)$ has a small error: $\mathbb{E} \left\{ L(\tilde{F}, \tilde{V}) \right\} \leq \nu$.

In the inductive model, the algorithm needs to estimate μ to a small error which is not possible with limited data $n \leq \frac{C\epsilon^2}{\log d} \sqrt{d \log \frac{1}{\nu}}$ (formally proved via a reduction to the lower bound in [25]). In the transductive model, the algorithm does not need to learn a function that works well for the whole distribution, but only need to search for one that works on x' . This allows to search in a much smaller set of hypotheses and requires less training data. In particular, we first use $\Theta(\log^2 \frac{1}{\nu})$ data in D to train a linear classifier $\text{sign}(\hat{\theta}^\top x)$ with a parameter $\hat{\theta}$. Upon receiving x' , we construct two large-margin classifiers: in the span of $\hat{\theta}$ and x' , find $\bar{\theta}_+$ and $\bar{\theta}_-$ that classify x' as $+1$ and -1 with a chosen margin, respectively. Finally, we use another set of $\Theta(\log^2 \frac{1}{\nu})$ data from D to check the two classifiers and pick the one with smaller errors. The picked classifier will classify x' correctly w.h.p., though it will not have a small error on the whole data distribution. Intuitively, the transductive model allows the algorithm to adapt to the given U and only search for hypotheses that can classify U correctly. Such adaptivity thus separates the two threat models.

C.3 Proof of Theorem 2

We prove this theorem by a series of lemmas. Let $n_0 := \sigma^4/d$, and choose K such $K \geq \Omega(\log \frac{1}{\nu})$ and $K \leq n_0$, e.g., $K = n_0$. Note that if $c \log^2 \frac{1}{\nu} \leq n \leq \frac{C\epsilon^2}{\log d} \sqrt{d \log \frac{1}{\nu}}$ for sufficiently large c and C , then we have $n_0 \geq K$ and $2Kn_0 \leq n \leq n_0 \cdot \frac{\epsilon^2 \sqrt{d/n_0}}{16 \log d}$.

Lemma 1 (Part (1)). *In the inductive threat model, the learned model $\tilde{F} = \Gamma(\mathcal{T}(D), D, U)$, by any algorithms \mathcal{T} and Γ , must have a large error:*

$$\mathbb{E} \left\{ L(\tilde{F}, \tilde{V}') \right\} \geq \frac{1}{2}(1 - d^{-1}) \geq \frac{1}{2}(1 - \nu), \quad (12)$$

where the expectation is over the randomness of D, V and possible algorithm randomness.

Proof. This follows from Corollary 23 in [25]. The only difference of our setting from theirs is that we additionally have unlabeled data U for the algorithm. Since the attacker can provide $x' = x$, the problem reduces to a problem with at most $n + 1$ data points in their setting, and thus the statement follows. \square

Transductive learning algorithms (\mathcal{T}, Γ) : To prove the statement (2), we give concrete learning algorithms that achieves small test error on x' . We consider learning a linear classifier $\text{sign}(\theta^\top x)$ with a parameter vector θ .

High-level structure of the learning algorithms. At the high level, the learning algorithms work as follows: At the training time we use part of the training data (denoted as D_2 to train a pretrained model $\bar{\theta}$), and part of the training data (denoted as D_1 , is reserved to test-time adaptation). Then, at the test time, upon receiving U , we use U to tune $\bar{\theta}$, and get two large-margin classifiers, $\bar{\theta}_+$ and $\bar{\theta}_-$, which classify x' as $+1$ and -1 , respectively. Finally, we check these two large margin classifiers on D_1 (that's where D_1 is used), and the one that generates smaller error wins and we classify x' into the winner class.

Detailed description. More specifically, the learning algorithms (\mathcal{T}, Γ) work as follows:

1. **Before game starts.** Let $m' = Kn_0, m = 10n_0$. We split the training set D into two subsets: $D_1 := \{(x_i, y_i)\}_{i=1}^{m'}$ and $D_2 := \{(x_{m'+i}, y_{m'+i})\}_{i=1}^m$. D_2 will be used to train a pretrained model at the training time, and D_1 will be used at the test time for adaptation.
2. **Training time.** \mathcal{T} uses the second part D_2 to compute a pretrained model, that is, a parameter vector:

$$\hat{\theta}_m = \frac{1}{m} \sum_{i=1}^m y_{m'+i} x_{m'+i}, \quad \bar{\theta} = \frac{\hat{\theta}_m}{\|\hat{\theta}_m\|_2}. \quad (13)$$

3. **Test time.** On input U, Γ uses D_1 and U to perform adaptation. At the high level, it adapts the pre-trained $\bar{\theta}$ along the direction of x' , such that it also has a large margin on x' , and also it makes correct predictions on D_1 with large margins. More specifically:

- (a) First, Γ constructs two classifiers, θ_+ and θ_- , such that θ_+ classifies x' to be +1 with a large margin, and θ_- classifies x' to be -1 with a large margin. Specifically:

$$\bar{x}' := x' / \|x'\|_2, \quad \gamma := \|x'\|_2 / 2, \quad (14)$$

$$\eta_+ := \frac{\gamma - (\bar{\theta})^\top x'}{\|x'\|_2}, \quad \theta_+ = \bar{\theta} + \eta_+ \bar{x}', \quad \bar{\theta}_+ = \theta_+ / \|\theta_+\|_2, \quad (15)$$

$$\eta_- := \frac{-\gamma - (\bar{\theta})^\top x'}{\|x'\|_2}, \quad \theta_- = \bar{\theta} + \eta_- \bar{x}', \quad \bar{\theta}_- = \theta_- / \|\theta_-\|_2. \quad (16)$$

where θ_+ and θ_- are viewed as the parameter vectors for linear classifiers. Note that θ_+ is constructed such that $\theta_+^\top x' / \|x'\|_2 = \gamma / \|x'\|_2 = 1/2$, and θ_- is such that $\theta_-^\top x' / \|x'\|_2 = -\gamma / \|x'\|_2 = -1/2$.

- (b) Finally, Γ checks their large margin errors on D_1 . Formally, let

$$t := \sigma \left(\sqrt{\frac{n_0}{d}} + \frac{n_0}{m} \right)^{-1/2}, \quad (17)$$

$$\text{err}_t(\theta) := \mathbb{E}_{(x,y)} \mathbb{I}[y\theta^\top x \leq t], \quad (18)$$

$$\widehat{\text{err}}_t(\theta) := \frac{1}{m'} \sum_{i=1}^{m'} \mathbb{I}[y_i \theta^\top x_i \leq t]. \quad (19)$$

If $\widehat{\text{err}}_t(\bar{\theta}_+) \leq \widehat{\text{err}}_t(\bar{\theta}_-)$, then Γ sets $\tilde{F}(x) := \text{sgn}(\bar{\theta}_+^\top x)$ and classifies x' to +1; otherwise, it sets $\tilde{F}(x) := \text{sgn}(\bar{\theta}_-^\top x)$ and classifies x' to -1.

Lemma 2 (Part (2)). *In the transductive threat model, for the \mathcal{T} and Γ described above, the adapted model $\tilde{F} = \Gamma(\mathcal{T}(D), D, U)$ has a small error:*

$$\mathbb{E} \left\{ L(\tilde{F}, \tilde{V}) \right\} \leq \nu. \quad (20)$$

Proof. Now, we have specified the algorithms and are ready to prove that w.h.p. $\tilde{F}(x')$ is the correct label y . By Lemma 3, $y(\text{err}_t(\bar{\theta}_-) - \text{err}_t(\bar{\theta}_+)) \geq \frac{c_4}{\sqrt{n_0}}$ with probability $\geq 1 - e^{-c_4 K}$. Then by the Hoeffding's inequality, D_1 is sufficiently large to ensure $y(\widehat{\text{err}}_t(\bar{\theta}_+) - \widehat{\text{err}}_t(\bar{\theta}_-)) > 0$ with probability $\geq 1 - 2e^{-c_4^2 K/2}$. This gives

$$\mathbb{E} \left\{ L(\tilde{F}, \tilde{V}) \right\} \leq e^{-cK}. \quad (21)$$

This is bounded by ν for the choice of K . □

Tools. We collect a few technical lemma below.

Lemma 3. *There exists absolute constants $c_4 > 0$ such that with probability $\geq 1 - e^{-c_4 K}$,*

$$y(\text{err}_t(\bar{\theta}_-) - \text{err}_t(\bar{\theta}_+)) \geq \frac{c_4}{\sqrt{n_0}}. \quad (22)$$

Proof. Without loss of generality, assume $y = +1$. The proof for $y = -1$ follows the same argument.

Note that

$$\text{err}_t(\theta) = \mathbb{E}_{(x,y)} \mathbb{I}[y\theta^\top x \leq t] \quad (23)$$

$$= \mathbb{P}(\mathcal{N}(\mu^\top \theta, \sigma^2 \|\theta\|_2^2) \leq t) \quad (24)$$

$$= Q\left(\frac{\mu^\top \theta - t}{\sigma \|\theta\|_2}\right), \quad (25)$$

where

$$Q(x) := \frac{1}{\sqrt{2\pi}} \int_x^{+\infty} e^{-t^2/2} dt. \quad (26)$$

First, consider $\bar{\theta}$.

$$\text{err}_t(\bar{\theta}) = Q\left(\frac{\mu^\top \bar{\theta} - t}{\sigma \|\bar{\theta}\|_2}\right) = Q(s), \text{ where } s := \frac{\mu^\top \bar{\theta} - t}{\sigma \|\bar{\theta}\|_2} = \frac{\mu^\top \bar{\theta} - t}{\sigma}. \quad (27)$$

By Lemma 4, we have with probability $\geq 1 - e^{-c_2(d/n_0)^{1/4} \min\{m, (d/n_0)^{1/4}\}}$,

$$\frac{\mu^\top \bar{\theta}}{\sigma \|\bar{\theta}\|_2} \leq \left(\sqrt{\frac{n_0}{d}} + \frac{n_0}{m}\right)^{-1/2} \left(1 + c_1 \left(\frac{n_0}{d}\right)^{1/8}\right), \quad (28)$$

$$\frac{\mu^\top \bar{\theta}}{\sigma \|\bar{\theta}\|_2} \geq \left(\sqrt{\frac{n_0}{d}} + \frac{n_0}{m}\right)^{-1/2} \left(1 - c_1 \left(\frac{n_0}{d}\right)^{1/8}\right), \quad (29)$$

which gives

$$s \leq c_1 \left(\frac{n_0}{d}\right)^{1/8} \left(\sqrt{\frac{n_0}{d}} + \frac{n_0}{m}\right)^{-1/2}, \quad (30)$$

$$s \geq -c_1 \left(\frac{n_0}{d}\right)^{1/8} \left(\sqrt{\frac{n_0}{d}} + \frac{n_0}{m}\right)^{-1/2}. \quad (31)$$

Since $m = 10n_0$ and $d \gg n_0$, we have

$$|s| = \left| \frac{\mu^\top \bar{\theta} - t}{\sigma \|\bar{\theta}\|_2} \right| \leq 1. \quad (32)$$

Next, we have

$$\text{err}_t(\theta_+) = Q\left(\frac{\mu^\top \bar{\theta}_+ - t}{\sigma \|\bar{\theta}_+\|_2}\right) = Q(s_+), \text{ where } s_+ := \frac{\mu^\top \bar{\theta}_+ - t}{\sigma \|\bar{\theta}_+\|_2} = \frac{\mu^\top \bar{\theta}_+ - t}{\sigma}, \quad (33)$$

$$\text{err}_t(\theta_-) = Q\left(\frac{\mu^\top \bar{\theta}_- - t}{\sigma \|\bar{\theta}_-\|_2}\right) = Q(s_-), \text{ where } s_- := \frac{\mu^\top \bar{\theta}_- - t}{\sigma \|\bar{\theta}_-\|_2} = \frac{\mu^\top \bar{\theta}_- - t}{\sigma}. \quad (34)$$

We now check the sizes of s_+ and s_- .

$$s_+ - s = \frac{\mu^\top \bar{\theta}_+ - t}{\sigma} - \frac{\mu^\top \bar{\theta} - t}{\sigma} \quad (35)$$

$$= \frac{\mu^\top \bar{\theta}_+ - \mu^\top \bar{\theta}}{\sigma} \quad (36)$$

$$= \frac{1}{\sigma \|\bar{\theta}_+\|_2} \left((1 - \|\bar{\theta}_+\|_2) \mu^\top \bar{\theta} + \eta_+ \mu^\top \bar{x}' \right). \quad (37)$$

Then by definition and bounds in Claim 1,

$$|s_+ - s| \leq \frac{2}{n_0} + 40 \leq 42. \quad (38)$$

Since $|s|$ is bounded by 1, we know $|s_+|$ is also bounded by 43. Similarly, $|s_- - s|$ and thus $|s_-|$ are also bounded by some constants. Furthermore,

$$s_+ - s_- = \frac{1}{\sigma} (\mu^\top \bar{\theta}_+ - \mu^\top \bar{\theta}_-) \quad (39)$$

$$= \frac{1}{\sigma} \left(\frac{\mu^\top \bar{\theta} + \eta_+ \mu^\top \bar{x}'}{\|\theta_+\|_2} - \frac{\mu^\top \bar{\theta} + \eta_- \mu^\top \bar{x}'}{\|\theta_-\|_2} \right). \quad (40)$$

By Claim 2, we have $\|\theta_-\|_2 = \|\theta_+\|_2$. Together with bounds in Claim 1, we have

$$s_+ - s_- = \frac{1}{\sigma \|\theta_+\|_2} (\eta_+ \mu^\top \bar{x}' - \eta_- \mu^\top \bar{x}') \quad (41)$$

$$= \frac{1}{\sigma \|\theta_+\|_2} (\eta_+ - \eta_-) \mu^\top \bar{x}' \quad (42)$$

$$= \frac{1}{\sigma \|\theta_+\|_2} \mu^\top \bar{x}' \quad (43)$$

$$\geq \frac{\sqrt{d}}{4\sigma^2} \quad (44)$$

$$= \frac{1}{4\sqrt{n_0}}. \quad (45)$$

Now we are ready to bound the error difference:

$$\text{err}_t(\bar{\theta}_-) - \text{err}_t(\bar{\theta}_+) = Q(s_-) - Q(s_+) \quad (46)$$

$$= \frac{1}{\sqrt{2\pi}} \int_{s_-}^{s_+} e^{-t^2/2} dt \quad (47)$$

$$\geq \frac{1}{\sqrt{2\pi}} (s_- - s_+) \times \min\{e^{-s_-^2/2}, e^{-s_+^2/2}\} \quad (48)$$

$$\geq \frac{c_4}{\sqrt{n_0}} \quad (49)$$

for some absolute constant $c_4 > 0$. □

Claim 1. *There exists a absolute constant $c_3 > 0$, such that with probability $\geq 1 - e^{-c_3 K}$,*

$$\sigma\sqrt{d}/4 \leq \|x'\|_2 \leq 2\sigma\sqrt{d}, \quad (50)$$

$$\frac{1}{2}\sigma \leq \frac{1}{4}\sigma\sqrt{\frac{m}{n_0}} \leq \bar{\theta}^\top \mu \leq 2\sigma\sqrt{\frac{m}{n_0}} \leq 10\sigma, \quad (51)$$

$$-\epsilon\sqrt{d}/2 \leq \bar{\theta}^\top x' \leq 2\epsilon\sqrt{d}, \quad (52)$$

$$d/2 \leq \mu^\top x' \leq 3d/2, \quad (53)$$

$$\frac{1}{2} - \frac{8\epsilon}{\sigma} \leq \eta_+ \leq \frac{1}{2} + \frac{8\epsilon}{\sigma}, \quad (54)$$

$$-\frac{1}{2} - \frac{8\epsilon}{\sigma} \leq \eta_- \leq -\frac{1}{2} + \frac{8\epsilon}{\sigma}. \quad (55)$$

Proof. First, since $x' = \mu + \sigma\zeta + \nu$ for $\zeta \sim \mathcal{N}(0, I)$, with probability $\geq 1 - e^{-c'd}$ for an absolute constant $c' > 0$, we have:

$$\sqrt{d}/2 \leq \|\zeta\|_2 \leq 3\sqrt{d}/2, \quad (56)$$

$$\|x'\|_2 \geq \sigma\sqrt{d}/2 - \|\mu\|_2 - \|\nu\|_2 \geq \sigma\sqrt{d}/4, \quad (57)$$

$$\|x'\|_2 \leq \sigma 3\sqrt{d}/2 + \|\mu\|_2 + \|\nu\|_2 \leq 2\sigma\sqrt{d}. \quad (58)$$

By Lemma 4, with probability $\geq 1 - e^{-c_2 K}$,

$$\bar{\theta}^\top \mu \leq 2\sigma \left(\sqrt{\frac{n_0}{d}} + \frac{n_0}{m} \right)^{-1/2} \leq 2\sigma \sqrt{\frac{m}{n_0}}, \quad (59)$$

$$\bar{\theta}^\top \mu \geq \frac{1}{2}\sigma \left(\sqrt{\frac{n_0}{d}} + \frac{n_0}{m} \right)^{-1/2} \geq \frac{\sigma}{4} \sqrt{\frac{m}{n_0}}. \quad (60)$$

Also, with probability $1 - e^{-c'K}$,

$$|\bar{\theta}^\top \zeta| \leq 2K\sigma. \quad (61)$$

Finally,

$$|\bar{\theta}^\top \nu| \leq \|\bar{\theta}\|_1 \|\nu\|_\infty \leq \epsilon\sqrt{d}. \quad (62)$$

Then

$$\bar{\theta}^\top x' = \bar{\theta}^\top (\mu + \sigma\zeta + \nu) \quad (63)$$

$$\leq |\bar{\theta}^\top \mu| + \sigma|\bar{\theta}^\top \zeta| + |\bar{\theta}^\top \nu| \quad (64)$$

$$\leq 2\sigma \sqrt{\frac{m}{n_0}} + 2K\sigma + \epsilon\sqrt{d} \quad (65)$$

$$\leq 2\epsilon\sqrt{d}. \quad (66)$$

and

$$\bar{\theta}^\top x' = \bar{\theta}^\top (\mu + \sigma\zeta + \nu) \quad (67)$$

$$\geq \sigma/2 - K\sigma - \epsilon\sqrt{d} \quad (68)$$

$$\geq -\epsilon\sqrt{d}/2. \quad (69)$$

For $\mu^\top x'$, we have with probability $\geq 1 - e^{-c'K}$,

$$\mu^\top x' = \mu^\top (\mu + \sigma\zeta + \nu) \quad (70)$$

$$\mu^\top x' \leq \|\mu\|_2^2 + 2K\sigma\|\mu\|_2 + \epsilon\|\mu\|_2\sqrt{d} \leq 3d/2, \quad (71)$$

$$\mu^\top x' \geq \|\mu\|_2^2 - 2K\sigma\|\mu\|_2 - \epsilon\|\mu\|_2\sqrt{d} \geq d/2. \quad (72)$$

By definition:

$$\eta_+ = \frac{1}{2} - \bar{\theta}^\top x' / \|x'\|_2, \quad (73)$$

so

$$\frac{1}{2} - 8\epsilon/\sigma \leq \eta_+ \leq \frac{1}{2} + 8\epsilon/\sigma. \quad (74)$$

Similarly,

$$-\frac{1}{2} - 8\epsilon/\sigma \leq \eta_- \leq -\frac{1}{2} + 8\epsilon/\sigma. \quad (75)$$

□

Claim 2.

$$\|\theta_+\|_2 = \|\theta_-\|_2. \quad (76)$$

Proof. We have by definition:

$$\|\theta_-\|_2^2 = \|\bar{\theta} + \eta_-\bar{x}'\|_2^2 \quad (77)$$

$$= 1 + \eta_-^2 + 2\eta_-\bar{\theta}^\top \bar{x}', \quad (78)$$

$$\|\theta_+\|_2^2 = \|\bar{\theta} + \eta_+\bar{x}'\|_2^2 \quad (79)$$

$$= 1 + \eta_+^2 + 2\eta_+\bar{\theta}^\top \bar{x}'. \quad (80)$$

Then

$$\|\theta_-\|_2^2 - \|\theta_+\|_2^2 = \eta_-^2 + 2\eta_-\bar{\theta}^\top \bar{x}' - \eta_+^2 - 2\eta_+\bar{\theta}^\top \bar{x}' \quad (81)$$

$$= (\eta_- - \eta_+)(\eta_- + \eta_+) + 2\bar{\theta}^\top \bar{x}'(\eta_- - \eta_+) \quad (82)$$

$$= (\eta_- - \eta_+)[(\eta_- + \eta_+) + 2\bar{\theta}^\top \bar{x}'] \quad (83)$$

$$= (\eta_- - \eta_+)[-2\bar{\theta}^\top \bar{x}'/\|\bar{x}'\|_2 + 2\bar{\theta}^\top \bar{x}'] \quad (84)$$

$$= 0. \quad (85)$$

This completes the proof. \square

Lemma 4 (Paraphrase of Lemma 1 in [5]). *Let $\hat{\theta}_m = \frac{1}{m} \sum_{i=1}^m y_i x_i$. There exist absolute constants c_0, c_1, c_2 such that for $\|\mu\|_2^2 = d, \sigma^2 = \sqrt{dn_0}$, and $d/n_0 > c_0$,*

$$\frac{\sigma^2 \|\hat{\theta}_m\|_2^2}{(\mu^\top \hat{\theta}_m)^2} \geq \left(\sqrt{\frac{n_0}{d}} + \frac{n_0}{m} \right) \left(1 - c_1 \left(\frac{n_0}{d} \right)^{1/8} \right), \quad (86)$$

$$\frac{\sigma^2 \|\hat{\theta}_m\|_2^2}{(\mu^\top \hat{\theta}_m)^2} \leq \left(\sqrt{\frac{n_0}{d}} + \frac{n_0}{m} \right) \left(1 + c_1 \left(\frac{n_0}{d} \right)^{1/8} \right), \quad (87)$$

with probability $\geq 1 - e^{-c_2(d/n_0)^{1/4} \min\{m, (d/n_0)^{1/4}\}}$.

D Experimental Details

D.1 General Setup

D.1.1 Computing Infrastructure

We run all experiments with PyTorch and NVIDIA GeForce RTX 2080Ti GPUs.

D.1.2 Dataset

We use three datasets GTSRB, MNIST, and CIFAR-10 in our experiments. The details about these datasets are described below.

GTSRB. The German Traffic Sign Recognition Benchmark (GTSRB) [27] is a dataset of color images depicting 43 different traffic signs. The images are not of a fixed dimensions and have rich background and varying light conditions as would be expected of photographed images of traffic signs. There are about 34,799 training images, 4,410 validation images and 12,630 test images. We resize each image to 32×32 . The dataset has a large imbalance in the number of sample occurrences across classes. We use data augmentation techniques to enlarge the training data and make the number of samples in each class balanced. We construct a class preserving data augmentation pipeline consisting of rotation, translation, and projection transforms

and apply this pipeline to images in the training set until each class contained 10,000 examples. We also preprocess images via image brightness normalization and normalize the range of pixel values to $[0, 1]$.

MNIST. The MNIST [20] is a large dataset of handwritten digits. Each digit has 5,500 training images and 1,000 test images. Each image is a 28×28 grayscale. We normalize the range of pixel values to $[0, 1]$.

CIFAR-10. The CIFAR-10 [18] is a dataset of 32×32 color images with ten classes, each consisting of 5,000 training images and 1,000 test images. The classes correspond to dogs, frogs, ships, trucks, etc. We normalize the range of pixel values to $[0, 1]$.

D.1.3 Implementation of Greedy Model Space Attack (GMSA)

We use the Projected Gradient Decent (PGD) [23] to solve the attack objective of GMSA. We apply PGD for each data point in V independently to compute the adversarial perturbation for the data point. For GMSA-AVG, at the i -th iteration, when applying PGD on the data point \mathbf{x} to generate the perturbation δ , we need to do one backpropagation operation for each model in $\{F^{(j)}\}_{j=0}^i$ per PGD step. So we do $i + 1$ times backpropagation in total. We do the backpropagation for each model sequentially and then accumulate the gradients to update the perturbation δ since we might not have enough memory to store all the models and compute the gradients at once, especially when i is large. For GMSA-MIN, at the i -th iteration, when applying PGD on the data point \mathbf{x} to generate the perturbation δ , we only need to do one backpropagation operation for the model $F^{(j^*)}$ with the minimum loss per PGD step. Here, $j^* = \arg \min_{0 \leq j \leq i} L(F^{(j)}, \mathbf{x} + \delta)$. We scale the number of PGD steps at the i -th iteration by a factor of $i + 1$ for GMSA-MIN so that it performs the same number of backpropagation operations as GMSA-AVG in each iteration.

D.2 Setup for URejectron Experiments

We use a subset of the GTSRB augmented training data for our experiments, which has 10 classes and contains 10,000 images for each class. We implement URejectron [11] on this dataset using the ResNet18 network [14] in the transductive setting. Following [11], we implement the basic form of the URejectron algorithm, with $T = 1$ iteration. That is we train a discriminator h to distinguish between examples from P and Q , and train a classifier F on P . Specifically, we randomly split the data into a training set D_{train} containing 63,000 images, a validation set D_{val} containing 7,000 images and a test set D_{test} containing 30,000 images. We then use the training set D_{train} to train a classifier F using the ResNet18 network. We train the classifier F for 10 epochs using Adam optimizer with a batch size of 128 and a learning rate of 10^{-3} . The accuracy of the classifier on the training set D_{train} is 99.90% and its accuracy on the validation set D_{val} is 99.63%. We construct a set \tilde{x} consisting of 50% normal examples and 50% adversarial examples. The normal examples in the set \tilde{x} form a set z . We train the discriminator h on the set D_{train} (with label 0) and the set \tilde{x} (with label 1). We then evaluate URejectron’s performance on \tilde{x} : under a certain threshold used by the discriminator h , we measure the fraction of normal examples in z that are rejected by the discriminator h and the error rate of the classifier F on the examples in the set \tilde{x} that are accepted by the discriminator h . The set z can be D_{test} or a set of corrupted images generated on D_{test} . We use the method proposed in [15] to generate corrupted images with the corruption type of brightness and the severity level of 1. The accuracy of the classifier on the corrupted images is 98.90%. The adversarial examples in \tilde{x} are generated by the PGD attack [23] or the CW attack [4]. For PGD attack, we use L_∞ norm with perturbation budget $\epsilon = 8/255$ and random initialization. The number of iterations is 40 and the step size is $1/255$. The robustness of the classifier under the PGD attack is 3.66%. For CW attack, we use L_2 norm as distance measure and set $c = 1$ and $\kappa = 0$. The learning rate is 0.01 and the number of steps is 100. The robustness of the classifier under the CW attack is 0.00%.

Dataset	Model	Accuracy	Robustness
MNIST	Standard	99.50	0.00
	Madry et al.	99.60	93.50
CIFAR-10	Standard	94.30	0.00
	Madry et al.	83.20	46.80

Table 4: Performance of the pre-trained models used by RMC. The robustness of the models is evaluated under the PGD attack. All values are percentages.

D.3 Setup for RMC Experiments

We follow the settings in [33] and perform experiments on MNIST and CIFAR-10 datasets to evaluate the adversarial robustness of RMC. Under our evaluation framework, RMC can be treated as an adaptation method Γ and the size of the test set U is 1 since RMC adapts the model based on a single data point. Suppose $V = \{(\hat{\mathbf{x}}, y)\}$, $U = \{\hat{\mathbf{x}}\}$ and the current model is F , then the loss of RMC on U is $L(\Gamma(U, F), V)$. Given a sequence of test inputs $(\hat{\mathbf{x}}^{(1)}, y^{(1)}), \dots, (\hat{\mathbf{x}}^{(n)}, y^{(n)})$, suppose the initial model is $F^{(0)}$, then the loss of RMC on the data sequence is $\frac{1}{n} \sum_{i=1}^n L(F^{(i)}, \hat{\mathbf{x}}^{(i)}, y^{(i)})$, where $F^{(i)} = \Gamma(F^{(i-1)}, \hat{\mathbf{x}}^{(i)})$. We assume that the attacker knows Γ and can use it to simulate the adaptation process to generate a sequence of adversarial examples $\hat{\mathbf{x}}^{(1)}, \dots, \hat{\mathbf{x}}^{(n)}$. Then we evaluate the robustness of RMC on the generated data sequence $\hat{\mathbf{x}}^{(1)}, \dots, \hat{\mathbf{x}}^{(n)}$.

We also evaluate RMC and RMC⁺ (an extended version of RMC) under the PGD-skip attack setting proposed in [33]: the attacker generates an adversarial example $\hat{\mathbf{x}}^{(p+1)}$ against the network that has been adapted to $\hat{\mathbf{x}}^{(1)}, \dots, \hat{\mathbf{x}}^{(p)}$. We follow their original setting for PGD-skip: first generate adversarial examples $\hat{\mathbf{x}}^{(1)}, \dots, \hat{\mathbf{x}}^{(p)}$ using the initial model $F^{(0)}$, and then generate the adversarial example $\hat{\mathbf{x}}^{(p+1)}$ on a clean input $\mathbf{x}^{(p+1)}$ randomly sampled from the test data distribution using the model $F^{(p)}$ that has been adapted to $\hat{\mathbf{x}}^{(1)}, \dots, \hat{\mathbf{x}}^{(p)}$. The robustness of RMC (or RMC⁺) is evaluated on $\hat{\mathbf{x}}^{(p+1)}$ using $F^{(p)}$. We repeat the experiment independently for 1000 times and calculate the average robustness. To save computational cost, we use the same $\hat{\mathbf{x}}^{(1)}, \dots, \hat{\mathbf{x}}^{(p)}$ for all independent experiments.

We consider two kinds of pre-trained models for RMC (or RMC⁺): one is the model trained via standard supervised training; the other is the model trained using the adversarial training proposed in [23]. The performance of the pre-trained models is shown in Table 4. We describe the settings for each dataset below.

D.3.1 MNIST

Model architecture and training configuration. We use a neural network with two convolutional layers, two full connected layers and batch normalization layers. For both standard training and adversarial training, we train the model for 100 epochs using the Adam optimizer with a batch size of 128 and a learning rate of 10^{-3} . We use the L_∞ norm PGD attack as the adversary for adversarial training with a perturbation budget ϵ of 0.3, a step size of 0.01, and number of steps of 40.

RMC and RMC⁺ configuration. We set $K = 1024$. Suppose the clean training set is \mathbb{D} . Let \mathbb{D}' contain $|\mathbb{D}|$ clean inputs and $|\mathbb{D}|$ adversarial examples. So $N' = 2|\mathbb{D}|$. We generate the adversarial examples using the L_∞ norm PGD attack with a perturbation budget ϵ of 0.3, a step size of 0.01, and number of steps of 100. We extract the features from the penultimate layer of the model and use the Euclidean distance in the feature space of the model to find the top-K nearest neighbors of the inputs. When adapting the model, we use Adam as the optimizer and set the learning rate to be 2×10^{-4} . We train the model until the early-stop condition holds. That is the training epoch reaches 100 or the validation loss doesn't decrease for 5 epochs. For RMC⁺, we use the same configuration, except that we update \mathbb{D}' using the model $F^{(p)}$ when evaluating it on $\mathbf{x}^{(p+1)}$.

Attack configuration. We use PGD to solve the attack objectives of all attacks used for our evaluation,

including FPA, GMSA-AVG, GMSA-MIN and PGD-skip. We use the same configuration for all attacks: L_∞ norm PGD with a perturbation budget ϵ of 0.3, a step size of 0.01, and number of steps of 100. We set $T = 9$ for FPA, GMSA-AVG and GMSA-MIN.

D.3.2 CIFAR-10

Model architecture and training configuration. We use the ResNet-32 network [14]. For both standard training and adversarial training, we train the model for 100 epochs using Stochastic Gradient Decent (SGD) optimizer with Nesterov momentum and learning rate schedule. We set momentum 0.9 and ℓ_2 weight decay with a coefficient of 10^{-4} . The initial learning rate is 0.1 and it decreases by 0.1 at 50, 75 and 90 epoch respectively. The batch size is 128. We augment the training images using random crop and random horizontal flip. We use the L_∞ norm PGD attack as the adversary for adversarial training with a perturbation budget ϵ of $8/255$, a step size of $2/255$, and number of steps of 10.

RMC and RMC⁺ configuration. We set $K = 1024$. Suppose the clean training set is \mathbb{D} . Let \mathbb{D}' contain $|\mathbb{D}|$ clean inputs and $4|\mathbb{D}|$ adversarial examples. So $N' = 5|\mathbb{D}|$. We generate the adversarial examples using the L_∞ norm PGD attack with a perturbation budget ϵ of $8/255$, a step size of $1/255$, and number of steps of 40. We extract the features from the penultimate layer of the model and use the Euclidean distance in the feature space of the model to find the top-K nearest neighbors of the inputs. We use Adam as the optimizer and set the learning rate to be 2.5×10^{-5} . For RMC⁺, we use the same configuration, except that we update \mathbb{D}' using the model $F^{(p)}$ when evaluating it on $\mathbf{x}^{(p+1)}$.

Attack configuration. We use PGD to solve the attack objectives of all attacks used for our evaluation, including FPA, GMSA-AVG, GMSA-MIN and PGD-skip. We use the same configuration for all attacks: L_∞ norm PGD with a perturbation budget ϵ of $8/255$, a step size of $1/255$, and number of steps of 40. We set $T = 9$ for FPA, GMSA-AVG and GMSA-MIN.

D.4 Setup for DANN and ATRM Experiments

We perform experiments on MNIST and CIFAR-10 datasets. We describe the settings for each dataset below.

D.4.1 MNIST

Model architecture. We use the same model architecture as the one used in [6], which is shown below.

Encoder
nn.Conv2d(3, 64, kernel_size=5)
nn.BatchNorm2d
nn.MaxPool2d(2)
nn.ReLU
nn.Conv2d(64, 128, kernel_size=5)
nn.BatchNorm2d
nn.Dropout2d
nn.MaxPool2d(2)
nn.ReLU
nn.Conv2d(128, 128, kernel_size=3, padding=1)
nn.BatchNorm2d
nn.ReLU
×2

Predictor	Discriminator
nn.Conv2d(128, 128, kernel_size=3, padding=1)	nn.Conv2d(128, 128, kernel_size=3, padding=1)
nn.BatchNorm2d	nn.ReLU
nn.ReLU	×5
×3	Flatten
flatten	nn.Linear(2048, 256)
nn.Linear(2048, 256)	nn.ReLU
nn.BatchNorm1d	nn.Linear(256, 2)
nn.ReLU	nn.Softmax
nn.Linear(256, 10)	
nn.Softmax	

Training configuration. We train the models for 100 epochs using the Adam optimizer with a batch size of 128 and a learning rate of 10^{-3} . We use the L_∞ norm PGD attack as the adversary to generate adversarial training examples with a perturbation budget ϵ of 0.3, a step size of 0.01, and number of steps of 40. For the representation matching in DANN and ATRM, we adopt the original progressive training strategy for the discriminator [10] where the weight α for the domain-invariant loss is initiated at 0 and is gradually changed to 0.1 using the schedule $\alpha = \frac{2}{1+\exp(-10 \cdot p)} - 1$, where p is the training progress linearly changing from 0 to 1.

Attack configuration. We use PGD to solve the attack objectives of all attacks used for our evaluation, including the transfer attack, FPA, GMSA-AVG, and GMSA-MIN. We use the same configuration for all attacks: L_∞ norm PGD with a perturbation budget ϵ of 0.3, a step size of 0.01, and number of steps of 200. We set $T = 9$ for FPA, GMSA-AVG and GMSA-MIN. When attacking DANN, we use the model trained via standard training as the initial model $F^{(0)}$ for the transfer attack, FPA and GMSA; when attacking ATRM, we use the model trained with adversarial training as the initial model $F^{(0)}$ for the transfer attack, FPA and GMSA.

D.4.2 CIFAR-10

Model architecture. We use the ResNet-18 network [14] and extract the features from the third basic block for representation matching. The detailed model architecture is shown below.

Encoder	Predictor	Discriminator
nn.Conv2d(3, 64, kernel_size=3)	BasicBlock(in_planes=512, planes=2, stride=2)	BasicBlock(in_planes=512, planes=2, stride=2)
nn.BatchNorm2d	avg_pool2d	avg_pool2d
nn.ReLU	flatten	flatten
BasicBlock(in_planes=64, planes=2, stride=1)	nn.Linear(512, 10)	nn.Linear(512, 2)
BasicBlock(in_planes=128, planes=2, stride=2)	nn.Softmax	nn.Softmax
BasicBlock(in_planes=256, planes=2, stride=2)		

Training configuration. We train the models for 100 epochs using stochastic gradient descent (SGD) optimizer with Nesterov momentum and learning rate schedule. We set momentum 0.9 and ℓ_2 weight decay with a coefficient of 10^{-4} . The initial learning rate is 0.1 and it decreases by 0.1 at 50, 75 and 90 epoch respectively. The batch size is 64. We augment the training images using random crop and random horizontal

flip. We use the L_∞ norm PGD attack as the adversary to generate adversarial training examples with a perturbation budget ϵ of $8/255$, a step size of $2/255$, and number of steps of 5. For the representation matching in DANN and ATRM, we adopt the original progressive training strategy for the discriminator [10] where the weight α for the domain-invariant loss is initiated at 0 and is gradually changed to 0.1 using the schedule $\alpha = \frac{2}{1+\exp(-10\cdot p)} - 1$, where p is the training progress linearly changing from 0 to 1.

Attack configuration. We use PGD to solve the attack objectives of all attacks used for our evaluation, including the transfer attack, FPA, GMSA-AVG, and GMSA-MIN. We use the same configuration for all attacks: L_∞ norm PGD with a perturbation budget ϵ of $8/255$, a step size of $1/255$, and number of steps of 100. We set $T = 9$ for FPA, GMSA-AVG and GMSA-MIN. When attacking DANN, we use the model trained via standard training as the initial model $F^{(0)}$ for the transfer attack, FPA and GMSA; when attacking ATRM, we use the model trained with adversarial training as the initial model $F^{(0)}$ for the transfer attack, FPA and GMSA.

D.5 Detailed Results for Attacking DANN and ATRM

Figure 2 shows the robustness of DANN and ATRM on the perturbed set $U^{(i)}$ generated by our attacks (FPA, GMSA-AVG, and GMSA-MIN) for each iteration i . Note that the robustness here is computed by the attacker with his randomness, which is different from the defender’s private randomness. The results show that usually FPA is not effective in attacking DANN and ATRM, and it cannot generate increasingly stronger attack sets over iterations. In attacking DANN, our GMSA-MIN attack is more effective and can generate increasing stronger attack sets over iterations while in attacking ATRM, our GMSA-AVG attack is more effective and can also generate increasing stronger attack sets over iterations. Compared to the robustness achieved by the defender shown in Table 3, we can see that by using private randomness, the defender may be able to achieve better robustness. For example, on MNIST, the robustness of DANN on the strongest attack set generated by GMSA-AVG is only 10.97%, but the defender can achieve 79.37% robustness on this attack set with his private randomness. This is because the attack set fails to attack the model space of the DANN defense (we observe that on this attack set, some previous models $F^{(i)}$ can achieve 71.28% robustness).

D.6 The Effect of Different Private Randomness for DANN and ATRM

We run the DANN and ATRM defense experiments five times with different random seeds on the same strongest attack set generated by our attacks (FPA, GMSA-AVG, and GMSA-MIN). The results in Figure 3 show that the robustness of DANN and ATRM doesn’t vary much with different private randomness.

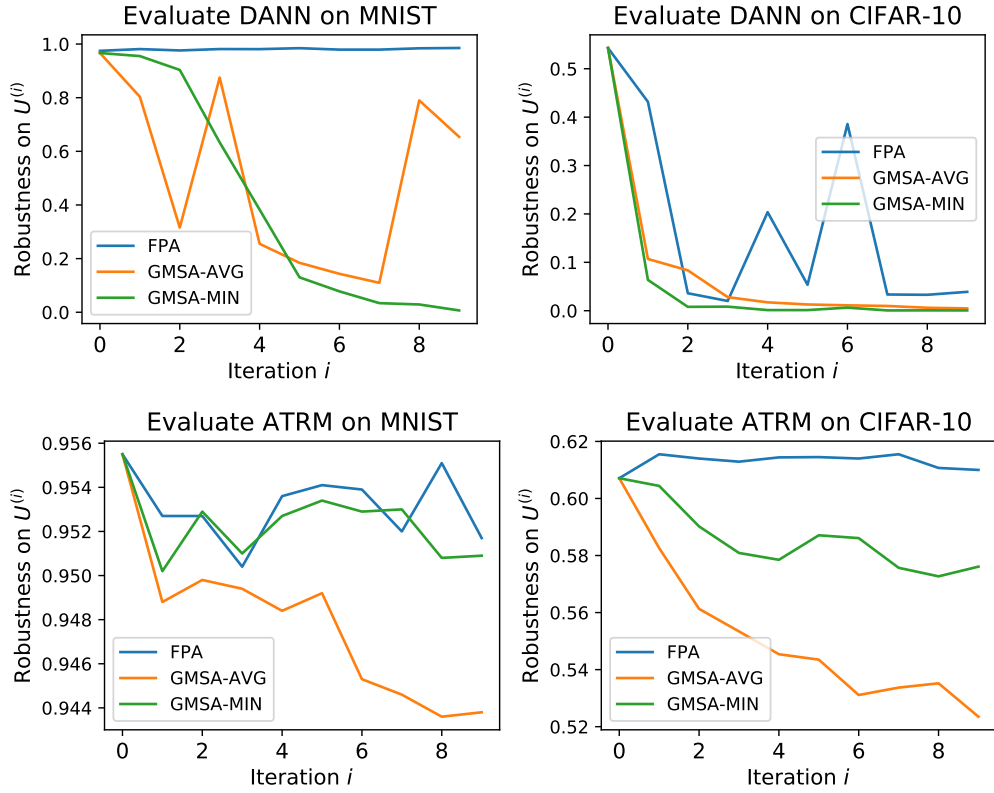


Figure 2: Detailed results for attacking DANN and ATRM on MNIST and CIFAR-10 using FPA, GMSA-AVG and GMSA-MIN attacks. The robustness of DANN (or ATRM) is evaluated by the attacker with his own randomness.

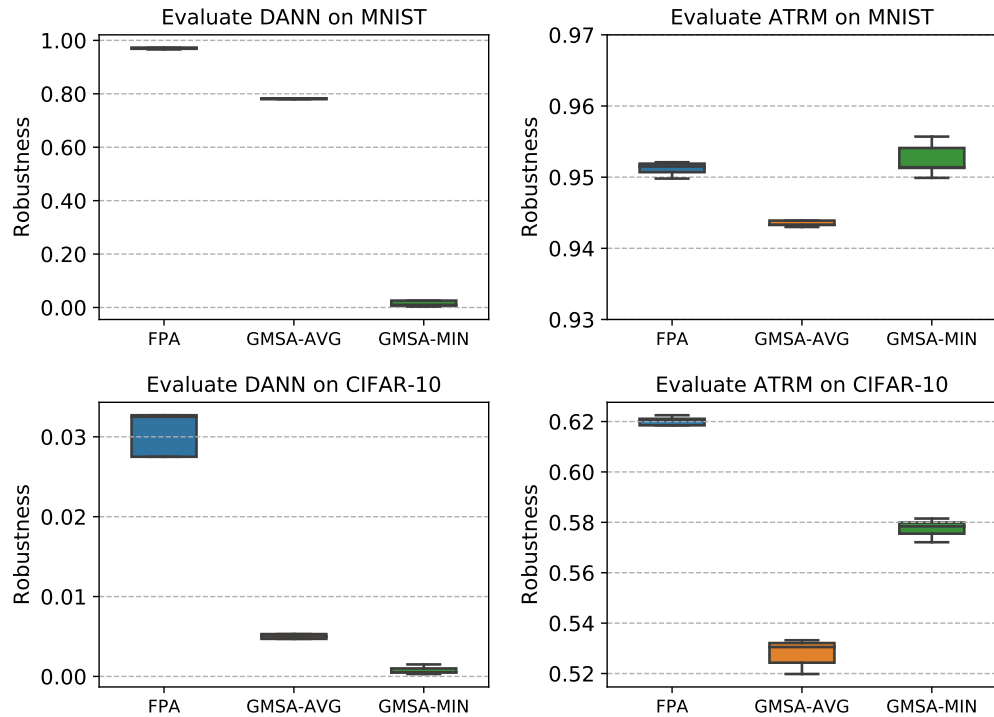


Figure 3: Multiple runs of DANN and ATRM defense experiments with different random seeds.